Adsorption of Weakly Charged Polyelectrolytes onto Oppositely Charged Spherical Colloids†

Roland G. Winkler*,‡ and Andrey G. Cherstvy§

Institut für Festkörperforschung, Forschungszentrum Jülich, D-52425 Jülich, Germany, and Max-Planck-Institut für Physik komplexer Systeme, Noethnitzerstraße 38, D-01187 Dresden, Germany

Received: December 11, 2006; In Final Form: March 5, 2007

The adsorption of a long weakly charged flexible polyelectrolyte in a salt solution onto an oppositely charged spherical surface is investigated. An analytical solution for Green's function is derived, which is valid for any sphere radius and consistently recovers the result of a planar surface in the limit of large sphere radii, by substituting the Debye−Hückel potential via the Hulthén potential. Expressions for critical quantities like the critical radius and the critical surface charge density are provided. In particular, we find a universal critical line for the sphere radius as a function of the screening length separating adsorbed from desorbed states. Moreover, results for the monomer density distribution, adsorbed layer thickness, and the radius of gyration are presented. A comparison of our theoretical results with experiments and computer simulations yields remarkably good agreement.

1. Introduction

The adsorption of polyelectrolytes onto charged surfaces is a fundamental process in biological systems and in a wide spectrum of technical applications. In nature, DNA−histone complexes are used as building blocks for compactification of genetic material in chromatin.[1−4] Complexes of DNA with oppositely charged objects, like spherical colloids/micelles or cylindrical micelles, are also extensively used in vitro for the purpose of gene therapy.[5−7] Industrial applications are as diverse as stabilization of colloidal suspensions, water treatment, and paper making.[8] Correspondingly, polyelectrolyte adsorption has been studied intensively experimentally, theoretically, and by computer simulations.

Despite significant efforts and progress, the understanding of charged complexes is still unsatisfactory and lags behind that of neutral complexes. This is partly due to the large number of parameters determining the properties of complexes—like the length of the polymer, its linear charge distribution and persistence length, the size, charge, and curvature of the complexed object, and the salt concentration to name the most important ones—which render the development of a comprehensive theory difficult. In addition, the long-range character of electrostatic interactions poses a significate theoretical challenge and exact analytical results are the exception rather than the rule.

During the past decade, a wealth of theoretical results have been presented and it is virtually impossible to address the achieved progress here. The spectrum of applied methods is wide and is often dictated by the particular aspect which the authors like to address. One of the first exact analytical studies for a planar surface was performed by Wiegel,[9] who analyzed the adsorption threshold and determined the properties of the adsorbed layer. Odijk[10] investigated the binding of polyelectrolytes to oppositely charged cylinders by a perturbation theory. Later, Muthukumar et al.[11,12] used a variational method to study the adsorption onto a planar, cylindrical, and spherical surface. In particular, Muthukumar[11] has taken into account the conformational changes of the polyelectrolyte upon variation of the salt concentration. The adsorption onto a spherical surface has been studied by a self-consistent variational approach by Haronska et al.[13] Finally, we recently presented exact analytical results for critical adsorption onto a sphere by replacing the Debye−Hückel potential via the Hulthén potential.[14,15] In addition, Linse and Shubin[16,17] used lattice models to study polyelectrolyte adsorption at planar oppositely charged surfaces. A scaling theory has been developed by Borisov et al.[18] and Dobrynin et al.[19] (see also refs 20 and 21 and references therein), which predicts strong conformational changes of the adsorbed polyelectrolytes when the surface charged density is varied. More specific models have been used to study the limit of strong polyelectrolyte adsorption. Here, the adsorption energy is large compared to the thermal fluctuations and the structure of the adsorbed polyelectrolyte is determined by the surface attraction and intramolecular repulsion rather than polyelectrolyte entropy. This leads to the formation of well-defined patters. In the case of spheres, tennis-ball patters,[22] rosettes,[23,24] or solenoids[15,22,25,26] have been predicted, whereas for cylinders helical structures[27−29] or strip patters have been suggested.[27] The investigated systems also diversify according to the polyelectrolyte flexibility. In various of the above references and others as well,[30−36] flexible chains are considered, whereas the influence of polymer persistence is addressed in refs 22−24 and 26−29.

Computer simulations—in particular Monte Carlo simulations—confirmed a number of the theoretical predictions. In a series of articles, Wallin and Linse[37−39] investigated the influence of chain flexibility, linear charge density, and sphere radius on the complexation of micelles. Akinchina and Linse[40] found transitions between tennis ball-like, solenoid, and rosettelike structures by varying the polyelectrolyte persistence length only.

† Part of the special issue "International Symposium on Polyelectrolytes (2006)".

* Corresponding author. E-mail: r.winkler@fz-juelich.de.
‡ Institute für Festkörperforschung.
§ Max-Planck-Institut.

10.1021/jp068489r CCC: $37.00
Published on Web 05/08/2007

Taking into account the intramolecular charge−charge interactions by a Debye−Hückel potential, Chodanowski and Stoll[41,42] and Kong and Muthukumar[43] undertook similar studies for the adsorption of polyelectrolytes onto spheres. These studies are of particular interest, because the results can directly be compared to theoretical predictions, which are often based on Debye−Hückel potentials too. Messina et al.[44,45] demonstrated that in the case of strong electrostatic coupling it is even possible to adsorb a polyelectrolyte with charges of the same sign as the sphere. In addition, the adsorption of polyelectrolytes onto oppositely charged planar surfaces has been studied by Yamakov et al.,[46] Ellis et al.,[47] and Messina,[48,49] who also considered the influence of image charges on adsorption.

Experimentally, similar studies of the influence of chain stiffness, colloid charge density, and salt concentration have been performed.[50−58] These studies revealed a number of differences when compared to theoretical results and computer simulations.

An interesting aspect in the adsorption of long polyelectrolytes onto oppositely charged surfaces, which was first found theoretically[9,11] and later confirmed experimentally,[50,57] is the appearance of a phase-transition-like behavior, i.e., a bound polymer state appears at critical conditions which depend on, e.g., the screening length ($1/\kappa$) of the Debye−Hückel potential, the temperature, or, in the case of adsorption onto a sphere, the sphere radius a. Experiments[50−58] suggest that the critical surface charge density σ_c increases as $|\sigma_c| \sim \kappa^b$, where $b = 1 - 1.4$, with increasing screening parameter κ. Both, flexible (polystyrensulfonate, PSS) and semiflexible (DNA) polymers have been used in experiments.[15] The variational calculations[11,12] could not account for the observed behavior mainly because the utilized ansatz applies to the limit of vanishing sphere curvature only. This has become clear from the solution of the adsorption problem exploiting the Hulthén potential[14] ($V_H \sim e^{-\kappa r}/(1 - e^{-\kappa r})$), which has provided exponents in agreement with experimental results when taking into account the dependence of the chain persistence length on the screening length.[11] The full solution of the adsorption problem[14] shows that the experimentally studied system sizes are in a crossover regime between the limits of strong and weak curvature ($\kappa a \approx 1 - 10$). Hence, it is essential to compare experimental results with the full solution of the adsorption problem in order to extract the influence of changes in various system properties upon changing the screening length. An example is the variation of the salt concentration, which changes not only the strength of the polyelectrolyte−sphere interaction but also the persistence length of the macromolecule. The comparison between experiments and theory suggests strong changes in the persistence length which naturally affect the adsorption behavior.[14,15]

In this article, we present results for the critical adsorption of a flexible polyelectrolyte onto an oppositely charged spherical surface. Expressions are provided, which are valid for any sphere radius and hence reproduce the results for a planar surface in the limit of vanishing sphere curvature. Particular emphasis is placed on the screening length dependence of the critical sphere radius. Our calculations provide a universal critical line for this radius,[14] and a detailed comparison yields excellent agreement with Monte Carlo simulations.[41] In comparison to refs 14 and 15, a more elaborate theoretical description is provided as well as an analysis of the polyelectrolyte radial distribution function, the thickness of the polyelectrolyte adsorption layer, and the polyelectrolyte conformational properties as a function of the sphere charge density and the Debye screening length. The comparison with Monte Carlo simulations reveals finite size effects in simulation results.

The paper is organized as follows. In section 2, the theoretical model is outlined and the solutions of the underlying differential equations are provided. The results are presented in section 3, and section 4 summarizes our findings.

2 Theoretical Description

2.1. Model. The polyelectrolyte is described by a continuous space curve with the linear charge density ρ. The intramolecular Coulomb and excluded volume interactions are not taken into account explicitly, but are rather adsorbed into the Kuhn segment of length l. Expressions for its dependence on the Debye screening length are provided in ref 12 (see also ref 59). Hence, we consider the limit of a weakly charged polyelectrolyte, where intramolecular charge−charge interactions perturb the polymer statistic only slightly. Taking counterions and salt ions into account by the Debye−Hückel potential, this corresponds to the limit where the Debye−Hückel potential among two Kuhn segments separated by l obeys $q^2 e^{-\kappa l}/\epsilon l \ll k_B T$ ($q = \rho l$). For $\kappa = 0$, this means $l_B/l \ll 1$, where l_B is the Bjerrum length. The oppositely charged macroion is considered a spherical particle of radius a with a homogeneous surface charge density σ. The solvent is accounted for by a medium of constant dielectric permittivity ϵ. The counterions and the present salt are taken into account on the level of the linearized Poisson−Boltzmann equation.[15] The ionic strength is constant everywhere outside of the sphere and is independent of the concentration of the adsorbing polyelectrolyte. References 60−62 provide examples of the ionic strength in solution dependent on the polyelectrolyte concentration with application to dense phases of DNA molecules. The solution of the linearized Poisson−Boltzmann equation yields the polymer−sphere interaction potential (Debye−Hückel potential[15]) per polymer length

$$V_{DH}(r) = -\frac{4\pi a^2 |\sigma\rho|}{\epsilon(1+\kappa a)} \frac{e^{-\kappa(r-a)}}{r} \tag{1}$$

where r is the radial distance from the sphere center.

The conformational properties of the flexible polyelectrolyte of length L and its spacial distribution of monomers follow from the probability density $G(r,r';L)$ (Green's function), where $r(0) = r'$ and $r(L) = r$ denote the positions of its end points. Green's function itself follows from the equation[9,11,63]

$$\left(\frac{\partial}{\partial L} - \frac{l}{6}\Delta_r + \frac{V(r)}{k_B T}\right) G(r, L|r', 0) = \delta(r - r')\delta(L) \tag{2}$$

with k_B the Boltzmann factor, T the temperature, and Δ_r the Laplace operator. V is the interaction potential per length, which is the Debye−Hückel potential (1) ($V = V_{DH}$). Equation 2 has to be solved with the boundary conditions $G = 0$ at the sphere surface and $\lim_{|r|\to\infty} G = 0$.

Unfortunately, no analytical solution of eq 2 with the Debye−Hückel potential has been found so far. In order to arrive at an analytical solution of the adsorption problem, we approximate the sphere potential by the Hulthén potential,[14,64] which yields

$$V(r) = V_H(r) = -\frac{4\pi a|\sigma\rho|(e^{\kappa a} - 1)}{\epsilon(1+\kappa a)} \frac{e^{-\kappa r}}{1 - e^{-\kappa r}} \tag{3}$$

This potential agrees with V_{DH} for $r \to a$. Moreover, the difference between the two potentials is small for $\kappa a \gg 1$, since r in the denominator is then slowly varying and can be replaced by a.

2.2. Determination of Green's Function. Since the Hulthén potential is spherically symmetric, we determine the solution of eq 2 by an expansion of G in terms of radial eigenfunctions $R_n(r)$ and the spherical harmonics $Y_{lm}(\varphi,\vartheta)$[9,11,63]

$$G(r,\varphi,\vartheta,L|r',\varphi',\vartheta',0) = \sum_{nlm} R_n(r)R_n(r')Y_{lm}(\varphi,\vartheta)Y^*_{lm}(\varphi',\vartheta')e^{-\lambda_{nlm}L} \quad (4)$$

For sufficiently large polymer lengths, the sum is dominated by the contribution of the ground state, i.e., $n = l = m = 0$. Hence, it is sufficient to study the equation for $R_0(r)$ which reads

$$\frac{l}{6}\left(\frac{\mathrm{d}^2R_0(r)}{\mathrm{d}r^2} + \frac{2}{r}\frac{\mathrm{d}R_0(r)}{\mathrm{d}r}\right) - \frac{V(r)}{k_BT}R_0(r) = -\lambda_0 R_0(r) \quad (5)$$

Before turning to a general solution of this equation, we consider the limit of a sphere with a small curvature, i.e., the limit $a \to \infty$. In this limit, the curvature term in eq 5 containing $1/r$ can be neglected and the Debye−Hückel interaction potential (1) (and also the Hulthén interaction potential) reduces to $V_{DH}(r) \approx -4\pi|\sigma\rho|e^{-\kappa a}e^{-\kappa r}/\kappa$. The differential eq 5 then becomes

$$\frac{l}{6}\frac{\mathrm{d}^2R_0(r)}{\mathrm{d}r^2} + \frac{4\pi|\sigma\rho|e^{-\kappa a}}{k_BT\epsilon\kappa}e^{-\kappa r}R_0(r) = -\lambda_0 R_0(r) \quad (6)$$

This is the equation of a polyelectrolyte in front of a planar surface, a problem studied in detail by Wiegel.[9] Hence, in the limit of vanishing curvature, the spherical system consistently turns into the planar system.

In order to obtain the full solution of the differential equation with the Hulthén potential, we introduce the substitution

$$R_0(r) = \frac{A}{r}e^{-\xi_0\kappa r}(1 - e^{-\kappa r})\chi(r) \quad (7)$$

and $x = 1 - e^{-\kappa r}$, where ξ_0 is related with λ_0 via $\lambda_0 = -l\xi_0^2\kappa^2/6$ (more details can be found in ref 15) and A is the normalization constant. Equation 5 then turns into the hypergeometric differential equation

$$x(1-x)\frac{\mathrm{d}^2}{\mathrm{d}x^2}\chi(x) + [2 - x(3 + 2\xi_0)]\frac{\mathrm{d}}{\mathrm{d}x}\chi(x) - \left(1 + 2\xi_0 - \frac{2}{p}\right)\chi(x) = 0 \quad (8)$$

for χ, with

$$p = \frac{\kappa^2\epsilon k_BTl(1+\kappa a)}{12\pi a|\sigma\rho|(e^{\kappa a} - 1)} \quad (9)$$

The solution of eq 8 around the point $x = 1$ is given by $\chi(x) = F(\alpha, \beta; \alpha + \beta - \gamma + 1; 1 - x)$ with F as the Gauss hypergeometric function ($_2F_1$) and the abbreviations $\alpha = \xi_0 + 1 - \sqrt{\xi_0^2 + 2/p}$, $\beta = \xi_0 + 1 + \sqrt{\xi_0^2 + 2/p}$, and $\gamma = 2$.[65] Since $F(\alpha, \beta; \alpha + \beta - \gamma + 1; 0)$ is finite and $\alpha + \beta - \gamma + 1$ is neither zero nor a negative integer, $R_0(r)$ in eq 7 satisfies the boundary condition for $r \to \infty$.

The eigenvalue λ_0 (or ξ_0) is determined from the boundary condition $R_0(a) = 0$. In general, the eigenvalues of eq 5 can be positive or negative.[9] The positive eigenvalues correspond to free states, since then $\xi_0 \sim \sqrt{-\lambda_0} \in \mathbb{C}\backslash\mathbb{R}$ and the eigenfunction is periodic. For eigenvalues $\lambda < 0$, bound states are present, because $\xi_0 \in \mathbb{R}$ and $R_0(r)$ decays exponentially for $r \to \infty$. The transition between free and bound states appears for $\lambda_0 = \xi_0 = 0$. The boundary condition $R_0(a) = 0$ yields then a particular value for $p = p_c(\kappa a)$. Since this value separates the adsorbed from the desorbed states of the polymer, we denote it as critical value p_c. With its help, we obtain a dependence of the critical adsorption temperature, critical sphere charge density, and critical sphere radius on the inverse Debye screening length κ.[14,15] Explicitly, the condition which determines p_c is given by

$$F(1 - \sqrt{2/p_c}, 1 + \sqrt{2/p_c}; 1; e^{-\kappa a}) = 0 \quad (10)$$

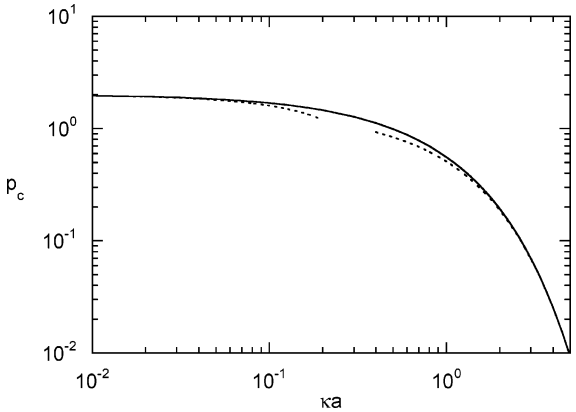

Figure 1. Critical values p_c obtained from the boundary condition at the sphere surface. Polyelectrolyte adsorption takes place for $p < p_c$. The dotted lines are the approximations $p_c \approx 2 - 4\kappa a$ for $\kappa a \ll 1$ and $p_c = (8/j_0^2)e^{-\kappa a}$, where $j_0 = 2.4048...$, for $\kappa a \gg 1$, respectively.

3 Results

3.1. Critical Adsorption. The numerical solution of eq 10 is presented in Figure 1. Polyelectrolyte adsorption takes place for $p < p_c$. The critical p_c exhibits a monotonic decrease with increasing κa. For small κa, it is well approximated by $p_c \approx 2 - 4\kappa a$. This dependence is consistent with the necessary condition for the existence of zeros for F, namely, $p < 2$.[66]

An analytical approximation for the "critical" function χ_c in the large curvature limit ($\kappa a \to 0$) is obtained in the following way: For large curvatures, the terms with the derivatives in eq 8 dominate its solution, i.e., the solution follows from the differential equation

$$x(1-x)\frac{\mathrm{d}^2}{\mathrm{d}x^2}\chi_c(x) + (2 - 3x)\frac{\mathrm{d}}{\mathrm{d}x}\chi_c(x) = 0 \quad (11)$$

which yields

$$\chi_c(r) = \chi_c^0\left(\frac{1}{e^{\kappa a} - 1} - \frac{1}{e^{\kappa r} - 1} + \ln\frac{e^{\kappa r} - 1}{e^{\kappa a} - 1}\right) \quad (12)$$

for $\kappa a \le \kappa r \to 0$. Equation 8 is then fulfilled for $p_c = 2$.

As discussed in the last section, in the small curvature limit ($\kappa a \to \infty$), the spherical adsorption problem turns into the problem of a polyelectrolyte in front of a charged planar surface. The corresponding eigenfunction and critical adsorption condition[9] follow also from the hypergeometric function. In the limit $\kappa a \to \infty$, the boundary condition (10) can be expressed in terms of Legendre functions of the first kind P_ν and the Bessel function of the first kind J_0 according to $\lim_{\kappa a\to\infty} F(\alpha_c, 2 - \alpha_c; 1; e^{-\kappa a}) = \lim_{\kappa a\to\infty} P_{-\alpha_c}(1 - 2e^{-\kappa a}) = \lim_{\kappa a\to\infty} J_0(\sqrt{8/p_c}e^{-\kappa a/2}) = 0$, with $\alpha_c = 1 - \sqrt{2/p_c}$.[65] The latter condition is identical to the boundary condition for critical adsorption onto a planar surface.[9,11,14] Denoting the first positive root of J_0 by j_0, where

$j_0 = 2.4048...$, we obtain the approximation $p_c = (8/j_0^2)e^{-\kappa a}$ for large κa. Figure 1, shows the agreement between this approximation and the full numerical solution of eq 10.

The critical p_c presented in Figure 1 is determined using the Hulthén potential rather than the Debye−Hückel potential. The above discussion demonstrates that in the small curvature limit the difference between the Debye−Hückel potential and the Hulthén potential vanishes. From the following considerations, it will be evident that the function $F_c(r) = F(1 - \sqrt{2/p_c}, 1 + \sqrt{2/p_c}; 1; e^{-\kappa r})$ provides the appropriate critical p_c for the Debye−Hückel potential in the limit $\kappa a \leq \kappa r \ll 1$ as well. Using the Debye−Hückel potential, eq 8 reads

$$x(1-x)\frac{d^2}{dx^2}\chi_c(x) + (2-3x)\frac{d}{dx}\chi_c(x) - \left(1 + \frac{2a\kappa x}{p_c \ln(1-x)(1-e^{-\kappa a})}\right)\chi_c(x) = 0 \quad (13)$$

Again, the first two terms are satisfied by the function (12) and the remaining part disappears at $r = a$ for $p_c = 2$. Hence, the critical value $p_c = 2$ is identical for the Hulthén and the Debye−Hückel potential in the limit $\kappa a \ll 1$ and $(r - a)/a \ll 1$.

The critical value p_c allows us to calculate other critical quantities for polyelectrolyte adsorption, such as the critical temperature,[11,15] the critical colloid surface charge density[14,15] σ_c, or the critical colloid radius a_c via eq 9. Results for the critical temperature and the critical surface charge density have been presented and discussed in refs 14 and 15. Thus, we summarize here our findings for σ_c only. Using the above limiting values for p_c, we obtain the following approximations

$$|\sigma_c| = \begin{cases} (\epsilon k_B T l/24\pi a^2|\rho|)\kappa, & \kappa a \ll 1 \\ (j_0^2 \epsilon k_B T l/96\pi|\rho|)\kappa^3, & \kappa a \gg 1 \end{cases} \quad (14)$$

The exact solution for the Debye−Hückel potential predicts a linear dependence of the critical colloid charge density on the inverse Debye screening length for $\kappa a \ll 1$. This is different from the predicted dependence $|\sigma_c| \sim \kappa^2$ based on the variational calculation of ref 12. However, the variational calculation of ref 13 predicts the same dependence on κ, but the numerical factor is rather different. The Kuhn segment length l of the polymer is independent of κ in this limit, as shown in ref 11. In the opposite limit of small curvature ($\kappa a \gg 1$), the obtained κ dependence is identical to that found by variational calculations.[12−14]

The limit $\kappa a \rightarrow \infty$ corresponds to the limit of a planar surface, and we obtain exactly the same expression as that derived for such a geometry in refs 9 and 11. However, these authors consider a planar surface with surface charge densities on both sides of the plane. The small curvature limit of our potential corresponds to a charge density on one of the surfaces only. This leads to a $|\sigma_c|$ which is a factor two larger than that presented in refs 9 and 11.

The analytical approximation for $\kappa a \ll 1$ (eq 14) not only predicts a critical surface charge density but also a critical colloid charge $Q_c = 4\pi a^2|\sigma_c| \sim \kappa$ itself. This implies that, for sufficiently small colloids, critical adsorption is independent of the size of the colloid; it only depends on κ.

So far, we assumed that the Kuhn length (or persistence length) is independent of the Debye screening length. It is, however, well-known that the persistence length of flexible polyelectrolytes exhibits a κ dependence. There exist various power-law predictions $l \sim \kappa^{-b_l}$ for such a dependence, with exponents in the range $b_l = {}^4/_5 - {}^6/_5$.[11,59,67,68] A detailed discussion of the κ dependence of the persistence length by far exceeds the focus of the current paper; we would however like to point out that recent simulations and scaling considerations[59,67,68] are in agreement with the original prediction $l \sim \kappa^{-2}$ by Odijk[69] and Skolnik and Fixman.[70] For our purpose, we use the definition of the projection length presented in ref 59 as a measure of persistence length, which exhibits the exponent $b_l = {}^6/_5$.

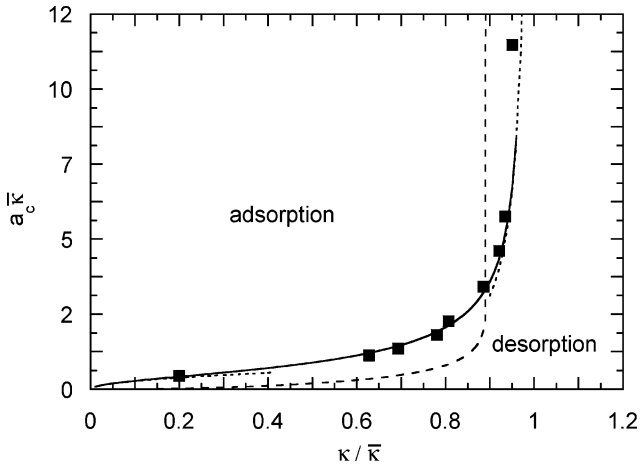

Figure 2. Critical radius a_c as a function of the Debye screening length according to eq 16. The dotted lines are the approximations of eq 17. The dashed line represents the critical radius according to the variational calculations of refs 12 and 43. The symbols are Monte Carlo simulation results taken from ref 41.

The complex formation of a polyelectrolyte with oppositely charged micelles and proteins has been studied in, e.g., refs 53, 54, and 56−58. These experiments confirm that complexation occurs only when the surface charge density exceeds a critical value, which typically grows with the reciprocal Debye screening length as $|\sigma_c| \sim \kappa^b$ with $b = 1 - 1.4$.[15,54,56−58] Our results agree with the experimental findings when we take the above κ dependence of l into account.[14,15]

Instead of the charge density σ_c, a critical sphere radius a_c can be determined[12,41,43] which separates adsorbed from the desorbed polyelectrolyte states. By introducing the abbreviation

$$\bar{\kappa} = \left(\frac{96\pi|\sigma\rho|}{j_0^2 \epsilon k_B T l}\right)^{1/3} \quad (15)$$

and using the definition (9), we obtain the following equation for a_c

$$p_c(\kappa a_c)(e^{\kappa a_c} - 1) - \frac{8\kappa^2}{j_0^2 a_c \bar{\kappa}^3}(1 + \kappa a_c) = 0 \quad (16)$$

Its solution yields a *universal* curve for $a_c\bar{\kappa}$ as a function of $\kappa/\bar{\kappa}$.

The numerical solution of eq 16 is shown in Figure 2 together with the analytical approximations

$$a_c\bar{\kappa} = \begin{cases} \sqrt{4\kappa/\bar{\kappa} j_0^2}, & \kappa \ll \bar{\kappa} \\ ((\kappa/\bar{\kappa})^2/(1 - (\kappa/\bar{\kappa})^3)), & \kappa \rightarrow \bar{\kappa} \end{cases} \quad (17)$$

No adsorption is obtained in the region located at the right of the curve. At a fixed $\kappa < \bar{\kappa}$, the entropy penalty due to adsorption of the chain monomers decreases with increasing sphere radius. Beyond the critical radius, the energy gain exceeds the entropy loss and the polymer adsorbs at the sphere surface. As is obvious

from the analytical expression, $\bar{\kappa}$ is the maximum value of the inverse Debye screening length; no adsorption is obtained for larger values neither for a sphere nor for a planar surface. This is qualitatively consistent with the variational calculations of refs 12 and 43. These calculations predict the same dependence of the maximum value of κ on the polymer and sphere parameters as our solution does. Quantitatively, however, the value of the variational calculation is smaller by the factor $8/j_0^2$. In addition, the shape of the critical curve is rather different as shown in Figure 2.

In ref 41, the adsorption of a polyelectrolyte onto a spherical particle has been studied by Monte Carlo simulations. In particular, the critical sphere radius has been determined as a function of κ. Aside from the interactions considered in our model, intramolecular charge−charge interactions have been taken into account by the Debye−Hückel potential as well as excluded volume interactions. As a consequence, the simulated systems exhibit significant conformational changes of the polymer when changing the Debye screening length. However, by examining the simulation results, in particular Figures 1 and 3 of ref 41 for the chain of $N = 100$ monomers, we conclude that the polyelectrolyte molecule exhibits nearly the same conformational behavior for κ values close to the adsorption transition independent of the colloidal radius ($\kappa \gtrsim 0.1$ 1/Å). Thus, a direct comparison of the theoretical with the simulation results is feasible.

By adjusting the κ values of the simulation data[41] such that the singularity appears at unity and multiplying the critical radii by an adequate factor, we achieve a remarkably good agreement with our universal a_c curve, as shown in Figure 2. This procedure yields the maximum κ value $\bar{\kappa}_s \approx 0.25$ 1/Å, i.e., the κ values of the simulations presented in Figure 2 are multiplied by 4.02 and the critical radii are divided by 16.16. The latter value is by a factor of 4 larger than expected. The difference might be related to the different applied adsorption criteria in ref 41 and our theoretical approach. We clearly expect a larger critical radius from the simulations, because in simulations a polymer is considered adsorbed when it is in contact with the particle for more than 50% of the simulation time during the minimization period,[41] whereas in our analytical approach adsorption is characterized by a transition from free to bound states (see the discussion at the end of section 2). Hence, the difference between the simulation data and the results of the variational calculations of the Muthukumar model is not due to the ground state dominance approximation as speculated in ref 41. It is rather a consequence of the limited applicability of the variational ansatz used in ref 12.

Using the simulation parameters presented in ref 41, eq 15 yields the maximum κ value 0.35 1/Å, when we use the Kuhn length $l = 7.14$ Å. This value is approximately 40 % larger than the above $\bar{\kappa}_s$ value. The difference is largely caused by a too small Kuhn length (persistence length). The excluded volume interactions and the electrostatic repulsion of the equally charged monomers lead to a swelling of the polyelectrolyte compared to the Gaussian chain used in the present calculations. An appropriate persistence length can partially account for this swelling. By using a factor of 2 larger Kuhn length, we find the maximum κ value ≈ 0.28 1/Å which is close to $\bar{\kappa}_s$, which demonstrates the correct trend.

3.2. Adsorbed Polyelectrolyte: Conformational Properties. We will now discuss the conformational properties of an adsorbed polyelectrolyte. We like to repeat once more that we neglect intramolecular charge−charge interactions. Hence, our approach does not apply to systems where such interactions give rise to particular polyelectrolyte patterns such as solenoids or tennis ball-like structures on the colloid surface. Nevertheless, we expect useful qualitative insight into the structure of the adsorbed polyelectrolyte layer for weakly charged polyelectrolytes.

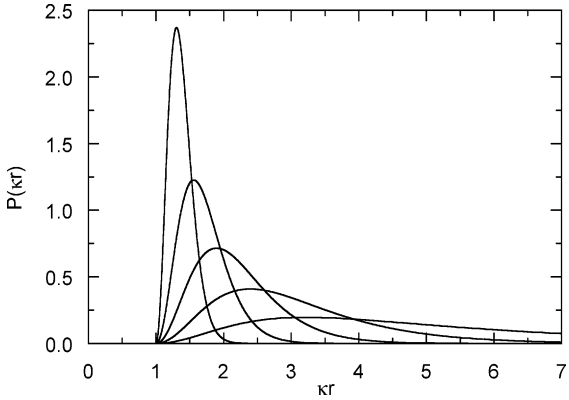

Figure 3. Radial monomer density distribution for $\kappa a = 1$ and the surface charge densities $\hat{\sigma} = 3$, 5, 10, 25, and 100 (from right to left) (cf. eq 20).

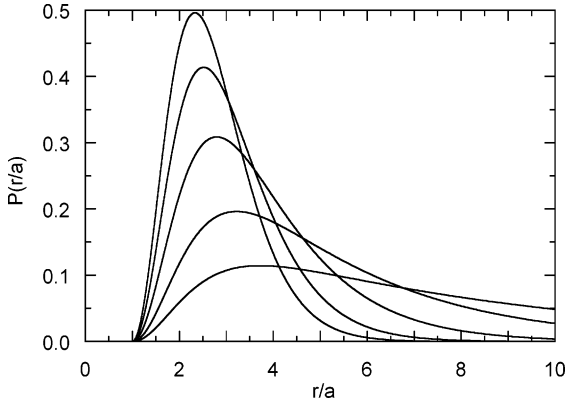

Figure 4. Radial monomer density distribution for the charge density $\hat{\sigma} = 3$ and the Debye−Hückel screening parameters $\kappa a = 0.1$, 0.5, 0.8, 1.0, and 1.1 (from left to right).

The radial eigenfunction for an adsorbed polyelectrolyte is given by eq 7 with $\xi_0 > 0$. The eigenvalue ξ_0 itself follows from the boundary condition

$$F(\xi_0 + 1 - \sqrt{\xi_0^2 + 2/p}, \xi_0 + 1 + \sqrt{\xi_0^2 + 2/p}; 2\xi_0 + 1; e^{-\kappa a}) = 0 \quad (18)$$

for a given $p < p_c$ (9). For small p values, multiple solutions of this equation are obtained, corresponding to the various "excited states".[71] The largest value ξ corresponds to the smallest eigenvalue λ_{nlm} and hence to the ground state. (A detailed discussion of the eigenvalues is presented in ref 15.)

Upon adsorption, a polyelectrolyte is confined in the vicinity of the spherical colloid. The degree to which it is confined is reflected in the radial monomer density, which is given by

$$P(r) = \frac{R_0(r)^2 r^2}{\int_a^\infty R_0(r)^2 r^2 \, dr} \quad (19)$$

in the ground state dominance approximation. Figures 3 and 4 provide examples of such distributions for various effective charge densities

$$\hat{\sigma} = 12\pi a^3|\sigma\rho|/(\epsilon k_B T l) \tag{20}$$

and Debye screening lengths, respectively. The $\hat{\sigma}$ values in Figures 3−5 cover the experimental range of colloid and polyelectrolyte parameters (see Figure 11 in ref 15). For the critical parameters, the density distribution P is very broad and reaches a finite value for $r \rightarrow \infty$. With increasing colloid surface charge density or decreasing κ,[16,17] the distribution becomes narrower and decays exponentially for large distances. In both cases, this increases the interaction strength between the colloid and the polyelectrolyte which naturally results in a stronger adsorption. Smaller spheres require larger $|\sigma|$ values for the polyelectrolyte adsorption to take place, as is evident from eq 14. The position of the peak shifts to larger radial distances with decreasing surface charge density and increasing κ, respectively. However, this change is small compared to the dramatic increase in the thickness of the adsorbed layer.

A measure for the thickness Δ of the adsorbed layer is the full width at half-height of the distribution function $P(r)$.[15] As shown in Figure 5, the adsorbed layer becomes more compact with increasing charge density $|\sigma|$ and decreasing κ at a given sphere radius a. Moreover, the width of the distribution diverges when κa approaches the critical value (see the inset of Figure 5). Scaling κa by $\hat{\sigma}^{2/5}$ seems to indicate an approximate linear decrease of $\kappa\Delta$ with respect to this reduced variable for all surface charge densities. This leads to the dependence

$$\Delta \sim a^{-1/5}|\sigma|^{-2/5} \tag{21}$$

of the layer thickness *far away* from the critical adsorption transition. A plot of the layer thickness as a function of the surface charge density for various κa values confirms these results, in particular the dependence for eq 21.

Scaling considerations predict the dependence $\Delta \sim |\sigma|^{-1/3}$ for the layer thickness of an adsorbed polyelectrolyte on a planar surface.[18−21] The results of Figure 5 are approximately consistent with this finding. Moreover, our results for a planar surface presented in ref 15 suggest the relation $\Delta_p \sim |\sigma|^{-3/8}$, which is also close to the scaling prediction.

The conformational properties of an adsorbed polyelectrolyte differ from those of a free polyelectrolyte.[41] To characterize the modifications, we determine its mean-square radius of gyration

$$r_g^2 = \int_a^\infty r^2 P(r)\, dr \tag{22}$$

Figure 6 shows r_g^2 as a function of the colloid radius for various Debye−Hückel parameters $\kappa/\bar{\kappa}$. The displayed nonmonotonic behavior is explained as follows: Close to the adsorption transition, the radius of gyration of the polyelectrolyte is almost identical to that of the free polymer. Since we consider an infinitely long polymer, r_g^2 diverges when $\bar{\kappa}a \rightarrow \bar{\kappa}a_c$. With increasing sphere radius, the width of the monomer distribution decreases very rapidly (see Figure 5) which causes the initial decrease of the radius of gyration. At larger a, the polymer is confined in a narrow layer close to the sphere surface and the width of the density distribution exhibits a weak dependence $\Delta \sim a^{-1/5}$ (21) on the sphere radius. An increase of the sphere radius causes then an increase of the layer radius which is not compensated for by a decrease in the layer thickness. Hence, the radius of gyration increases with increasing a again. The shift of the curves in Figure 6 to larger r_g^2 and $\bar{\kappa}a$ with increasing $\kappa/\bar{\kappa}$ is explained by the reduced attraction of the polyelectrolyte at larger κ.

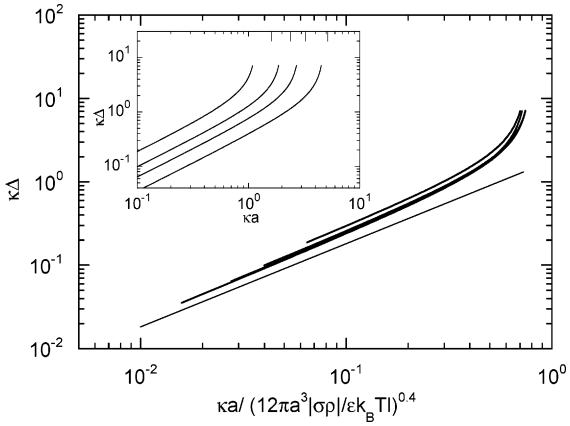

Figure 5. Thickness of the adsorbed polyelectrolyte layer for the charge densities $\hat{\sigma} = 3$, 10, 25, and 100 (from top to bottom). The straight line has a slope of 1. In the inset, the maximum κa values are indicated on the upper x axis.

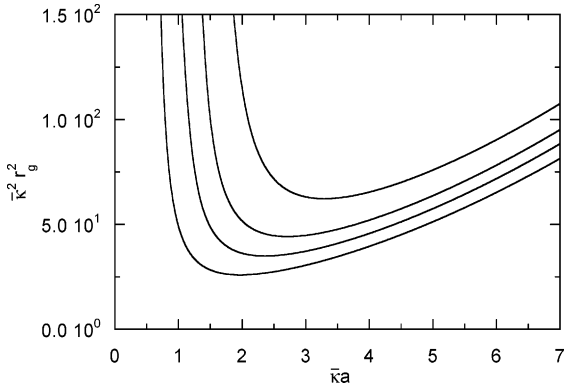

Figure 6. Mean-square radius of gyration of an adsorbed polyelectrolyte as a function of the sphere radius for the Debye−Hückel parameters $\kappa/\bar{\kappa} = 0.3$, 0.5, 0.6, and 0.7 (left to right). $\bar{\kappa}$ is given in eq 15.

Qualitatively, the theoretically obtained dependence of the radius of gyration on the sphere radius is in agreement with the simulation results of refs 41 and 43. There, also an initial decrease and a later increase of the radius of gyration is found. However, the results cannot be compared quantitatively for several reasons. On the one hand, we did not take into account the conformational changes of the polyelectrolyte due to intramolecular charge−charge interactions. Our results apply as long as the conformational changes by such interactions are small. On the other hand, we consider an infinitely long polyelectrolyte. The results of Figures 3 and 4 of ref 41 demonstrate that polyelectrolyte finite size effects might be important in an adsorption process. A polyelectrolyte chain of finite length can be completely adsorbed on a sphere for a certain polymer length to radius ratio (cf Table 2 of ref 41). As a consequence, the radius of gyration is mainly determined by the sphere size and to a lesser extent by the screening length. Then, r_g^2 is independent of the salt concentration as show in Figures 3 and 4 of ref 41. The situation is different for an infinitely long polymer, which is not able to cover a finite size sphere by a monolayer (or less than a monolayer) only. Here, larger κ values will lead to larger layer thicknesses and larger radii of gyration.

It has been suggested that polyelectrolytes get trapped in the vicinity of a sphere, when the attraction energy of a monomer exceeds the penalty of its entropic confinement ($\sim k_B T$) close to the sphere.[51,58] This region of high potential around the sphere should become thinner as κ increases, because the electrostatic

potential decays faster away from the sphere, and the region should become larger with increasing sphere charge density. Thus, larger $|\sigma|$ values would be required to form polyelectrolyte−sphere complexes at higher salt concentrations. Clearly, this statement is qualitatively consistent with our analytical result (14). Using the same crude model as in ref 51, however, leads to a completely different dependence of the critical charge density on κ, namely $|\sigma_c| \sim (\kappa a + 1)$.[51] This yields a far to weak dependence on κ for $\kappa a \gg 1$, and σ_c is independent of κa for $\kappa a \ll 1$. These differences reflect the different underlying physical adsorption mechanisms. In the first case, it is assumed that the gain in adsorption energy compensates for the loss in translational entropy (of either some part of the polymer or the colloid), neglecting any conformational entropy changes. In our approach, however, conformational entropy changes play the dominate role—adsorption is achieved when the gain in adsorption energy compensates the loss in conformational entropy. Even for very small colloids is the spacial distribution of monomers rather different from that of a polyelectrolyte in free space (cf. Figures 4 and 5), particularly due to the boundary condition on the colloid surface. Thus, the presence of the colloid always affects the conformational properties of the polyelectrolyte. The adsorption process is governed by the polyelectrolyte conformational entropy rather than translational entropy (of some segments or the colloid) which we of course account for by using eq 2 as a starting point of our considerations.

In principle, we can determine the mean Debye−Hückel attraction energy per polymer length (1). This energy decreases with decreasing κ, because the monomer distribution becomes narrower. Interestingly, at the transition from an adsorbed to a desorbed state, the average energy is zero, because the critical eigenfunction is decaying very slowly with increasing radial distance and cannot be normalized. As a consequence, the polyelectrolyte fraction close to the sphere becomes zero when the desorption transition is approached.

4. Conclusions

We have studied the adsorption of a weakly charged flexible polyelectrolyte onto an oppositely charged spherical surface. A full solution for the Green's function of the polymer is obtained by replacing the Debye−Hückel potential via the Hulthén potential.

Considering the critical adsorption behavior, we determined a critical surface charge density and a critical sphere radius, respectively. The critical surface charge density exhibits a linear dependence on the Debye screening parameter κ for small sphere radii and turns into the previously predicted dependence for planar surfaces in the limit of large κa.[9,12] For the critical sphere radius, we obtain a universal curve which separates adsorbed from desorbed states. Monte Carlo simulation results[41] for this quantity are in excellent agreement with the theoretical prediction. This is surprising at first glance because the intramolecular excluded volume and charge−charge interactions have been neglected in the theoretical model and one might expect that the (strongly) charged polyelectrolyte of the Monte Carlo simulations exhibits considerable conformational changes when the salt concentration is changed. Considering the simulation data, however, it seems that the polyelectrolytes exhibit almost the same conformations close to the adsorption transition independent of the sphere radius and the salt concentration (cf. Figure 3 of ref 41). It is this similarity in the conformational properties near the critical point in the simulations which allows us to compare the simulation results for highly charged systems with those of our theoretical model for weakly charged polyelectrolytes. As far as the simulations are concerned, it would be interesting to extend the critical adsorption studies beyond the chain lengths examined in ref 41 to study the influence of finite size effects on critical adsorption and to verify or falsify our predicted universal critical curve.

Investigations of the radial monomer distribution show that the monomer layer thickness decreases with increasing surface charge density and decreasing screening parameter κ due to the increasing interaction strength. The analysis of the layer thickness yields an approximate scaling relation $\Delta \sim |\sigma|^{-2/5}$, which is close to the prediction for a planar surface ($\Delta \sim |\sigma|^{-3/8}$) and that obtained by scaling theory ($\Delta \sim |\sigma|^{-1/3}$),[18,19] far away from the critical values of polyelectrolyte adsorption.

Our considerations apply for long and flexible polyelectrolytes. In experiments, often polyelectrolyte adsorption onto spherical particles is considered, where the polyelectrolyte persistence length is larger than the sphere radius. For such systems, it is desirable to know the influence of the persistence length on the adsorption behavior. Thus, we encourage more advanced theoretical adsorption studies based on semiflexible polyelectrolyte models.

An important issue of polyelectrolyte adsorption is overcharging of a spherical object. Several theoretical models predict such an effect,[26,29,35,36,72,73] and it has been observed experimentally in complexation of polyelectrolytes with globular proteins of inhomogeneous charge patterns.[54] We have not addressed this issue in the current article; however, our results may help to resolve the critically discussed appropriate choice for the radial distribution function[36,72,74] for overcharging of a pointlike colloidal particle. Instead of the Coulomb potential, the Hulthén potential could be used in this description in the limit $\kappa a \rightarrow 0$, where we have shown that the same result for the Debye−Hückel and the Coulomb potential can be obtained. Extending the equation for the Green's function by a self-consistency term[13,36] and using the solution (7) in, e.g., a variational calculation might provide an appropriate solution for the overcharging problem.

Aside from that, we hope that our results stimulate further experimental studies of critical adsorption, in particular with respect to the predicted universal critical line for the sphere radius.

References and Notes

(1) Alberts, B.; Bray, D.; Lewis, J.; Raff, M.; Roberts, K.; Watson, J. D. *Molecular Biology of the Cell*; Garland: New York, 1994.
(2) Volkenstein, M. V. *Molecular Biophysics;* Academic Press: New York, 1977.
(3) Luger, K.; Mäder, A. M.; Richmond, R. K.; Sangent, D. F.; Richmond, T. J. *Nature (London)* **1997**, *389*, 251.
(4) Cherstvy, A. G.; Everaers, R. *J. Phys.: Cond. Matter* **2006**, *18*, 11429.
(5) Rädler, J. O.; Koltover, I.; Salditt, T.; Safinya, C. R. *Science* **1997**, *275*, 810.
(6) Gössl, I.; Shu, L.; Schlüter, A. D.; Rabe, J. P. *J. Am. Chem. Soc.* **2002**, *124*, 6860.
(7) Safinya, C. R.; Ewert, K.; Ahmad, A.; Evans, H. M.; Raviv, U.; Needleman, D. J.; Lin, A. J.; Slack, N. L.; George, C.; Samuel, C. E. *Philos. Trans. R. Soc. A* **2006**, *364*, 2573.
(8) Napper, D. H. *Polymeric Stabilization of Colloidal Dispersions*; Academic Press: New York, 1983.
(9) Wiegel, F. W. *J. Phys. A: Math. Gen.* **1977**, *10*, 299.
(10) Odijk, T. *Macromolecules* **1980**, *13*, 1542.
(11) Muthukumar, M. *J. Chem. Phys.* **1987**, *86*, 7230.
(12) van Goeler, F.; Muthukumar, M. *J. Chem. Phys.* **1994**, *100*, 7796.
(13) Haronska, P.; Vilgis, T. A.; Grottenmüller, R.; Schmidt, M. *Macromol. Theory Simul.* **1998**, *7*, 241.
(14) Winkler, R. G.; Cherstvy, A. G. *Phys. Rev. Lett.* **2006**, *96*, 066103.
(15) Cherstvy, A. G.; Winkler, R. G. *J. Chem. Phys.* **2006**, *125*, 064904.
(16) Linse, P. *Macromolecules* **1996**, *29*, 326.

(17) Shubin, V.; Linse, P. *Macromolecules* **1997**, *30*, 5944.
(18) Borisov, O. V.; Zhulina, E. B.; Birshtein, T. M. *J. Phys. II* **1994**, *4*, 913.
(19) Dobrynin, A. V.; Deshkovski, A.; Rubinstein, M. *Macromolecules* **2001**, *34*, 3421.
(20) Netz, R. R.; Andelman, D. *Phys. Rep.* **2003**, *380*, 1.
(21) Dobrynin, A. V.; Rubinstein, M. *Prog. Polym. Sci.* **2005**, *30*, 1049.
(22) Kunze, K.-K.; Netz, R. R. *Phys. Rev. Lett.* **2000**, *85*, 4389.
(23) Schiessel, H.; Rudnick, J.; Bruinsma, R.; Gelbart, W. M. *Europhys. Lett.* **2000**, *51*, 237.
(24) Schiessel, H. *Macromolecules* **2003**, *36*, 3424.
(25) Marky, N. L.; Manning, G. S. *Biopolymers* **1991**, *31*, 1543.
(26) Netz, R. R.; Joanny, J.-F. *Macromolecules* **1999**, *32*, 9026.
(27) Kunze, K.-K.; Netz, R. R. *Europhys. Lett.* **2002**, *58*, 299.
(28) Cherstvy, A. G.; Winkler, R. G. *J. Chem. Phys.* **2004**, *120*, 9394.
(29) Cherstvy, A. G.; Winkler, R. G. *J. Phys. Chem. B* **2005**, *109*, 2962.
(30) Ngyuen, T. T.; Shklovskii, B. I. *J. Chem. Phys.* **2001**, *114*, 5905.
(31) Ngyuen, T. T.; Shklovskii, B. I. *J. Chem. Phys.* **2001**, *115*, 7298.
(32) Ngyuen, T. T.; Shklovskii, B. I. *Physica A* **2001**, *293*, 324.
(33) Allen, R. J.; Warren, P. B. *Langmuir* **2004**, *20*, 1997.
(34) Park, S. Y.; Bruinsma, R. F.; Gelbart, W. M. *Europhys. Lett.* **1999**, *46*, 454.
(35) Mateescu, E. M.; Jeppesen, C.; Pincus, P. *Europhys. Lett.* **1999**, *46*, 493.
(36) Gurovitch, E.; Sens, P. *Phys. Rev. Lett.* **1999**, *82*, 339.
(37) Wallin, T.; Linse, P. *Langmuir* **1996**, *12*, 305.
(38) Wallin, T.; Linse, P. *J. Phys. Chem.* **1996**, *100*, 17873.
(39) Wallin, T.; Linse, P. *J. Phys. Chem. B* **1997**, *101*, 5506.
(40) Akinchina, A.; Linse, P. *Macromolecules* **2002**, *35*, 5183.
(41) Chodanowski, P.; Stoll, S. *J. Chem. Phys.* **2001**, *115*, 4951.
(42) Stoll, S.; Chodanowski, P. *Macromolecules* **2002**, *35*, 9556.
(43) Kong, C. Y.; Muthukumar, M. *J. Chem. Phys.* **1998**, *109*, 1522.
(44) Messina, R.; Holm, C.; Kremer, K. *Phys. Rev. E* **2001**, *65*, 041805.
(45) Messina, R.; Holm, C.; Kremer, K. *J. Chem. Phys.* **2002**, *117*, 2947.
(46) Yamakov, V.; Milchev, A.; Borisov, O.; Dünweg, B. *J. Phys.: Condens. Matter* **1999**, *11*, 9907.
(47) Ellis, M.; Kong, C. Y.; Muthukumar, M. *J. Chem. Phys.* **2000**, *112*, 8723.
(48) Messina, R. *Phys. Rev. E* **2004**, *70*, 051802.
(49) Messina, R. *Phys. Rev. E* **2006**, 74, 049906(E).
(50) Dubin, P. L.; Thé, S. S.; McQuigg, D. W.; Chew, C. H.; Gan, L. M. *Langmuir* **1989**, *5*, 89.
(51) McQuigg, D. W.; Kaplan, J. I.; Dubin, P. L. *J. Phys. Chem.* **1992**, *96*, 1973.
(52) Dubin, P. L., Bock, J., Davis, R. M., Schulz, D., Eds.; *Macromolecular Complexes in Chemistry and Biology*; Springer-Verlag: Berlin, 1994.
(53) Li, Y.; Dubin, P. L.; Spindler, R.; Tomalia, D. A. *Macromolecules* **1995**, *28*, 8426.
(54) Mattison, K. W.; Dubin, P. L.; Brittain, I. J. *J. Phys. Chem. B* **1998**, *102*, 3830.
(55) Xia, J. L.; Dubin, P. L.; Kokufuta, E.; Havel, H.; Muhoberac, B. B. *Biopolymers* **1999**, *50*, 7128.
(56) Miura, N.; Dubin, P. L.; Moorefield, C. N.; Newkome, G. R. *Langmuir* **1999**, *15*, 4245.
(57) Zhang, H.; Ohbu, K.; Dubin, P. L. *Langmuir* **2000**, *16*, 9082.
(58) Feng, X. H.; Dubin, P. L.; Zhang, H. W.; Kirton, G. F.; Bahadur, P.; Parotte, J. *Macromolecules* **2001**, *34*, 6373.
(59) Ullner, M. *J. Phys. Chem. B* **2003**, *107*, 8097.
(60) Poghossian, A.; Cherstvy, A. G.; Ingebrandt, S.; Offenhäusser, A.; Schöning, M. J. *Sens. Actuators, B* **2005**, *111*−*112*, 470.
(61) Cherstvy, A. G.; Kornyshev, A. A.; Leikin, S. *J. Phys. Chem. B* **2004**, *108*, 6508.
(62) Cherstvy, A. G.; Kornyshev, A. A.; Leikin, S. *J. Phys. Chem. B* **2002**, *106*, 13362.
(63) Doi, M.; Edwards, S. F. *The Theory of Polymer Dynamics*; Oxford University: Oxford, 1986.
(64) Lam, C. S.; Varshni, Y. P. *Phys. Rev. A* **1971**, *4*, 1875.
(65) Gradshteyn, I. S.; Ryzhik, I. M. *Table of Integrals, Series, and Products*; Academic Press Inc.: San Diego, 1980.
(66) Gil, A.; Koepf, W.; Segura, J. *Numer. Algorithms* **2004**, *36*, 113.
(67) Everaers, R.; Milchev, A.; Yamakov, V. *Eur. Phys. J. E* **2002**, *8*, 3.
(68) Nguyen, T. T.; Shklovskii, B. I. *Phys. Rev. E* **2002**, *66*, 021801.
(69) Odijk, T. *J. Polym. Sci. Polym. Phys. Ed.* **1977**, *15*, 477.
(70) Skolnik, J.; Fixman, M. *Macromolecules* **1977**, *10*, 944.
(71) For bound states, the eigenfunctions with $n = 0$ describe polyelectrolyte profiles with a single maximum at some distance from the sphere; integers $n > 1$ correspond to R_n functions which describe oscillating polymer profiles away from the sphere having $n - 1$ zeros. These solutions correspond to higher "energy" eigenvalues. Functions with nonzero l, m describe polyelectrolyte adsorption on a non-homogeneously charged "patchy" surface that can be applied for studying polyelectrolyte adsorption on real globular proteins with quite nonuniform charge patterns; see refs 15 and 75.
(72) Golestanian, R. *Phys. Rev. Lett.* **1999**, *83*, 2473.
(73) Nguyen, T. T.; Shklovskii, B. I. *J. Chem. Phys.* **2001**, *115*, 7298.
(74) Sens, P. *Phys. Rev. Lett.* **1999**, *83*, 2474.
(75) Cooper, C. L.; Goulding, A.; Kayitmazer, A. B.; Ulrich, S.; Stoll, S.; Turksen, S.; Yusa, S.; Kumar, A.; Dubin, P. L. *Biomacromolecules* **2006**, *7*, 1025.